

This article was downloaded by: [Siauliu University Library]

On: 17 February 2013, At: 07:01

Publisher: Taylor & Francis

Informa Ltd Registered in England and Wales Registered Number: 1072954 Registered office: Mortimer House, 37-41 Mortimer Street, London W1T 3JH, UK



Advanced Composite Materials

Publication details, including instructions for authors and subscription information:

<http://www.tandfonline.com/loi/tacm20>

Energy absorption in composite grid structures

Ronald F. Gibson

Version of record first published: 02 Apr 2012.

To cite this article: Ronald F. Gibson (2005): Energy absorption in composite grid structures, *Advanced Composite Materials*, 14:2, 113-119

To link to this article: <http://dx.doi.org/10.1163/1568551053970636>

PLEASE SCROLL DOWN FOR ARTICLE

Full terms and conditions of use: <http://www.tandfonline.com/page/terms-and-conditions>

This article may be used for research, teaching, and private study purposes. Any substantial or systematic reproduction, redistribution, reselling, loan, sub-licensing, systematic supply, or distribution in any form to anyone is expressly forbidden.

The publisher does not give any warranty express or implied or make any representation that the contents will be complete or accurate or up to date. The accuracy of any instructions, formulae, and drug doses should be independently verified with primary sources. The publisher shall not be liable for any loss, actions, claims, proceedings, demand, or costs or damages whatsoever or howsoever caused arising directly or indirectly in connection with or arising out of the use of this material.

Keynote lecture of the 30th anniversary of the JSCM

Energy absorption in composite grid structures

RONALD F. GIBSON *

*Mechanical Engineering Department, Advanced Composites Research Laboratory,
Wayne State University, Detroit, MI 48202, USA*

Received 3 September 2004; accepted 5 November 2004

Keywords: Composite grids; energy absorption; thermoplastic composites.

GREETINGS FROM THE AMERICAN SOCIETY FOR COMPOSITES

As president of the American Society for Composites (ASC) for 2004–2005, Professor Gibson is honored and delighted to present this paper, and he brings with him the best wishes of ASC to JSCM for a successful 30th anniversary symposium. It has been a great pleasure for ASC to co-sponsor the Japan–US Conference on Composite Materials with JSCM over the years, and we hope that the tradition will continue for many years to come. ASC will celebrate its 20th anniversary at its 2005 conference at Drexel University in Philadelphia, and we invite you all to join us there.

1. INTRODUCTION

This paper summarizes results from an analytical/experimental study of the energy absorption characteristics of grid-stiffened composite structures under transverse loading. Tests and finite element simulations were carried out for quasi-static loading of isogrid E-glass/polypropylene panels in 3-point bending. Test panels were fabricated by using a thermoplastic stamping process and co-mingled E-glass/polypropylene yarns. The results of the tests and simulations show that these types of structures have excellent energy absorption characteristics, and that most of the energy absorption occurs beyond initial failure. Results for isogrid panels loaded on the skin side will be compared with similar results for loading on the rib side, and conclusions regarding design of such structures for energy absorption will be offered.

*E-mail: gibson@eng.wayne.edu

Geodesic grid structures have a long and illustrious history, including the famous geodesic domes of Buckminster Fuller and the damage tolerant Wellington bombers of World War II [1]. These early grid structures typically consisted of wood or metal grid frames and fabric skins, but in recent years it has been found that grids consisting of unidirectional composite ribs can be used to great advantage [2–4]. So far, the use of grid-stiffened composite structures has been mainly restricted to relatively high cost, low volume aerospace applications such as launch vehicles [5] and orbital satellites [6], but there appears to be considerable potential for their use in low cost, high volume applications such as automotive vehicles and civil infrastructure. Thermoplastic stamping has been shown to be a fast and effective means of fabricating low cost composite grid structures [7]. Good impact energy absorption is a requirement in many of these potential applications such as door and floor panels in automotive vehicle structures and bridge decks in civil infrastructure.

The objective of the current research is to fabricate composite grid panels using a low cost thermoplastic stamping process and to evaluate their energy absorption characteristics under transverse loading using both 3-point bending tests and finite element simulations.

2. EXPERIMENTAL

Isogrid panel specimens with ribs oriented at angles of $0 \pm 60^\circ$ were fabricated by thermoplastic stamping in a specially grooved steel mold (Fig. 1) following the procedure outlined by Goldsworthy and Hiel [7].

Overall panel dimensions were 304 mm \times 264 mm, the rib cross-sectional dimensions were 6.36 mm \times 6.36 mm and the skin thickness was 1.28 mm. The composite material used was Vetrotex Twintex E-glass/polypropylene (PP), which consists of co-mingled E-glass reinforcing fibers and polypropylene matrix fibers. The ribs in the grids were made of unidirectional Twintex.Eglass/PP roving and the skins were made of woven Twintex.E-glass/PP. The co-mingled unidirectional E-glass/PP fibers were hand laid-up into grooves of the steel mold

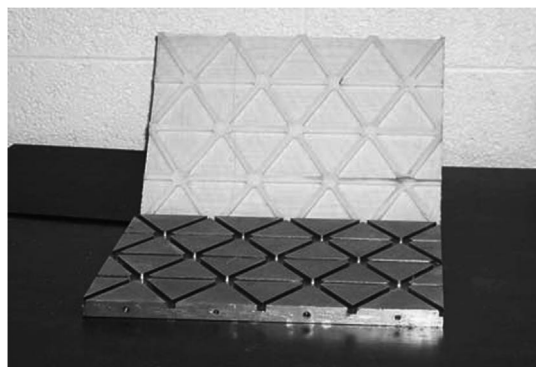


Figure 1. Isogrid panel specimen and mold.

to form the ribs of the isogrid patterns, then four layers of woven fabric Twintex[®] were layered on top of the ribs to form the skin. The mold with the composite layup was then placed in a TMP Composite Vacuum Press and molded under vacuum at 415F for 10 min with 65 psi mold pressure and 5 min with 195 psi mold pressure, then cooled to room temperature at 195 psi pressure, after which the vacuum was released. The fiber volume fractions in all ribs were controlled by counting the number of rovings in each groove and using the same number for all samples. Since it is very difficult to lay-up enough roving in the grooves to keep the fiber volume fraction of the ribs at a reasonable level in a one-step process, a multiple step fabrication procedure was used. First, ten pieces of roving were laid into every groove of the steel mold and then molded to form an isogrid or square grid. Second, the resulting grid was removed from the mold and another ten pieces of roving were wound into each groove of the mold, then the previously molded grid was placed on the top and the new grid was molded. A new isogrid with higher fiber volume fraction was thus fabricated. By repeating the above steps three times, the desired fiber volume fraction of 0.45 was obtained. The four-layer balanced woven fabrics of the same materials were comolded to form an isogrid stiffened plate specimen.

As shown in Fig. 2, the isogrid panel specimens were loaded in 3-point bending in a Enduratec SmartTest servopneumatic testing machine operating in displacement control at a rate of 0.05 mm/s.

The support span was 255 mm and a transverse line load was applied at midspan with a steel bar loading fixture. Energy absorption was characterized by plotting load–displacement curves and calculating the specific energy absorption (SEA) as the non-recoverable area under the load–displacement curve beyond initial failure divided by the loaded mass of the specimen between the supports. Failure modes associated with various features of the load–displacement curves were observed and recorded during the tests. In separate experiments, loading was applied on the rib side and on the skin side for comparison of energy absorption and associated failure modes.

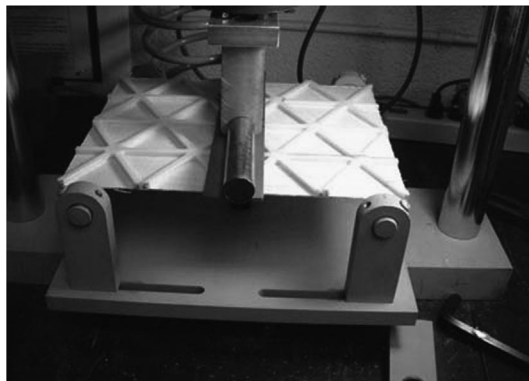


Figure 2. Test setup for 3-point bending.

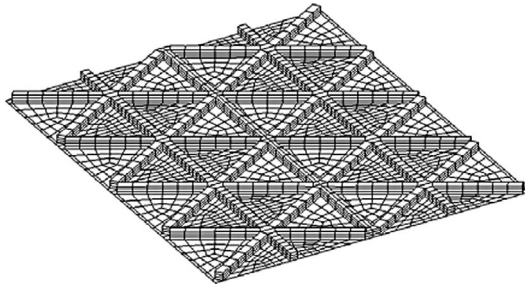


Figure 3. Finite element model of isogrid panel.

3. FINITE ELEMENT SIMULATIONS

For comparison with experimental results, numerical simulations were generated by using HYPERMESH for mesh generation and ABAQUS for the finite element analysis. 3D solid elements (type C3D8) were used to model the ribs and 2D shell elements (type S4) were used to model the skin. A typical finite element model having 2832 elements is shown in Fig. 3.

Elastic constants of the unidirectional rib material were estimated by using micromechanics models, while those of the woven skin were provided by Vetrotex. Longitudinal tensile and compressive strengths of the unidirectional rib material were found from 3-point bending tests of unidirectional beams similar to the ribs, while the corresponding transverse strengths were estimated from micromechanics. Strengths of the woven skin material were provided by Vetrotex.

A FORTRAN subroutine was implemented within the ABAQUS code to incorporate the material failure models. The user subroutine picks up the stress components of each element for each increment, and substitutes them into the appropriate failure criterion. The Maximum Stress Criterion was used for 3D solid ribs and the combined stress criterion based on Chang–Lessard model was used for the skin. If no damage has been found, the program proceeds to a new load step. However, if any failure is detected, the program iterates the current solution with the degraded properties until the nonlinear equations of equilibrium are satisfied. An exponential decay rule was used to ensure convergence following initial and subsequent failures. The degradation rate parameter affects damage front propagation within the material. The rate at which the material degrades determines the propagation of the damage front and therefore the spreading of the load to the surrounding material. Further details on the finite element simulations can be found in the dissertation by Gan [8].

4. RESULTS AND COMPARISONS

Figure 4 shows a typical comparison of experimental load–displacement results for one isogrid panel loaded on the rib side and for another similar panel loaded on the

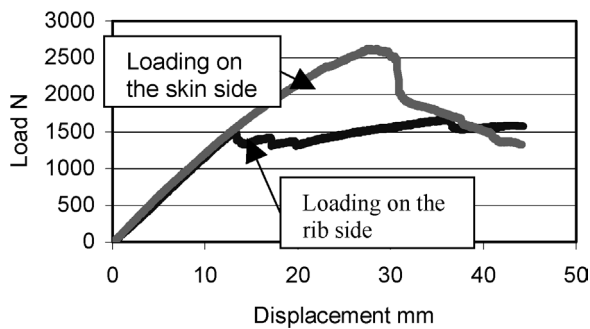


Figure 4. Comparison of measured load–displacement curves for isogrid panel loaded on the rib side with corresponding results for a similar panel loaded on the skin side.

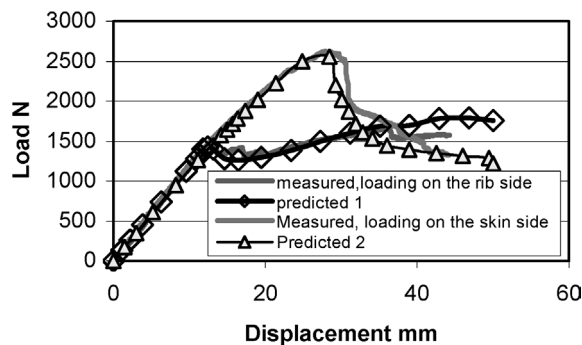


Figure 5. Predicted and measured responses for isogrid panels loaded on the rib side or the skin side.

skin side, while Fig. 5 shows a comparison of predicted and measured results for the two panels.

The maximum displacement of about 43 mm was limited by the test apparatus and complete failure of the specimens was not observed.

It is seen that the behavior beyond initial failure is quite different for the two loading conditions. For loading on the rib side, sequential local compressive failures of ribs by microbuckling led to a series of relatively small load drops. However, for loading on the skin side, local tensile failures (fiber breakage) in the ribs and skin buckling led to a substantial load drop following the peak load. The specific energy absorption values for the two cases are compared in Fig. 6, where it is seen that the SEA for the case of loading on the skin side is higher than that of loading on the rib side. It is important to remember, however, that the SEA corresponding to complete failure is unknown in both cases, and the load following initial failure seems to remain at a reasonably constant level and even increases slightly for the case loading on the rib side, whereas the load is trending downward following a sharp load drop after initial failure for loading on the skin side. So it is believed that the SEA at final failure will be larger for loading on the rib side than for loading on the skin side. Predicted and measured values of the specific strain energy at initial failure are also given in Fig. 6, and the agreement between predicted and measured

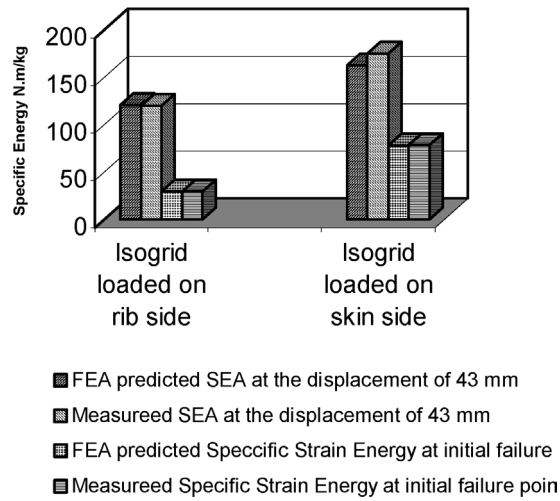


Figure 6. Comparison of predicted and measured energy absorption for isogrid panels loaded on rib side and skin side.

values is seen to be reasonable for both SEA and specific strain energy. Additional results for square grid structures and sandwich structures may be found in the dissertation by Gan [8]. For example, unlike the grid structures, foam core sandwich structures of similar size under similar transverse loading were observed to exhibit catastrophic failures and corresponding sharp load drops without development of a stable progressive damage process.

5. CONCLUDING REMARKS

Transverse load–displacement relationships and the corresponding energy absorption characteristics of thermoplastically stamped Eglass/polypropylene composite isogrid structures have been studied using both quasi-static 3-point bending tests and corresponding finite element simulations. Due to displacement limitations of the test apparatus, it was not possible to achieve complete failure of the test specimens, but observations within the limited displacement range led to some important conclusions. When transverse loading is applied on the rib side, once the peak load is achieved, a stable damage progression process develops, and this process consists of a sequence of relatively small load drops (and in some cases, slight increases in the load) corresponding to local compressive microbuckling of the ribs. When the transverse loading is applied on the skin side, however, the load drop after the peak load is much larger, and the load continues to drop due to the lack of a stable damage progression process. Although the SEA based on the 43 mm maximum displacement was greater for loading on the skin side, it is believed that if complete failure can be achieved, the maximum SEA will occur for loading on the rib side. Finite element simulations of progressively damaged isogrids show reasonable agreement with experiments.

Acknowledgements

The author gratefully acknowledges the contributions of Dr. Changsheng Gan and Dr. Golam Newaz and the support of the Wayne State University Institute for Manufacturing Research at Wayne State University.

REFERENCES

1. L. W. Rehfield, A brief history of analysis methodology for grid-stiffened geodesic composite structures, in: *Proc. 44th Intl. SAMPE Symposium*, on CD-ROM (1999).
2. H. Chen and S. W. Tsai, Analysis and optimum design of composite grid structures, *J. Compos. Mater.* **30**, 503–534 (1996).
3. S. Huybrechts and S. W. Tsai, Analysis and behavior of grid structures, *Compos. Sci. Technol.* **56**, 1001–1015 (1996).
4. Y. Chen and R. F. Gibson, Analytical and experimental studies of composite isogrid structures with internal passive damping, *Mech. Adv. Mater. Struct.* **10**, 127–143 (2003).
5. P. M. Wegner and J. E. Higgins, Compressive response of grid-stiffened structures having thin face sheets, in: *Proc. 10th US–Japan Conference on Composite Materials*, F. K. Chang (Ed.), pp. 925–930 (2002).
6. S. E. Hahn and T. Ozaki, Thermal and structural requirements for grid-stiffened satellite structures, in: *Proc. 10th US–Japan Conference on Composite Materials*, F. K. Chang (Ed.), pp. 909–916 (2002).
7. W. B. Goldsworthy and C. Hiel, Thermoplastics technology applied to manufacturing of grid-stiffened structures, in: *Proc. 44th Intl. SAMPE Symposium*, on CD-ROM (1999).
8. C. Gan, Behavior of grid-stiffened composite structures under transverse loading, PhD Dissertation, Wayne State University (2003).